

Fabrication and low temperature thermoelectric properties of Na_xCoO_2 ($x = 0.68$ and 0.75) epitaxial films by the reactive solid-phase epitaxy

W. J. Chang, C. C. Hsieh, T. Y. Chung, S. Y. Hsu, K. H. Wu, T. M. Uen, J.-Y. Lin, J. J. Lin, C.-H. Hsu, Y. K. Kuo, H. L. Liu, M. H. Hsu, Y. S. Gou, and J. Y. Juang

Citation: *Applied Physics Letters* **90**, 061917 (2007); doi: 10.1063/1.2437131

View online: <http://dx.doi.org/10.1063/1.2437131>

View Table of Contents: <http://scitation.aip.org/content/aip/journal/apl/90/6?ver=pdfcov>

Published by the [AIP Publishing](#)

Articles you may be interested in

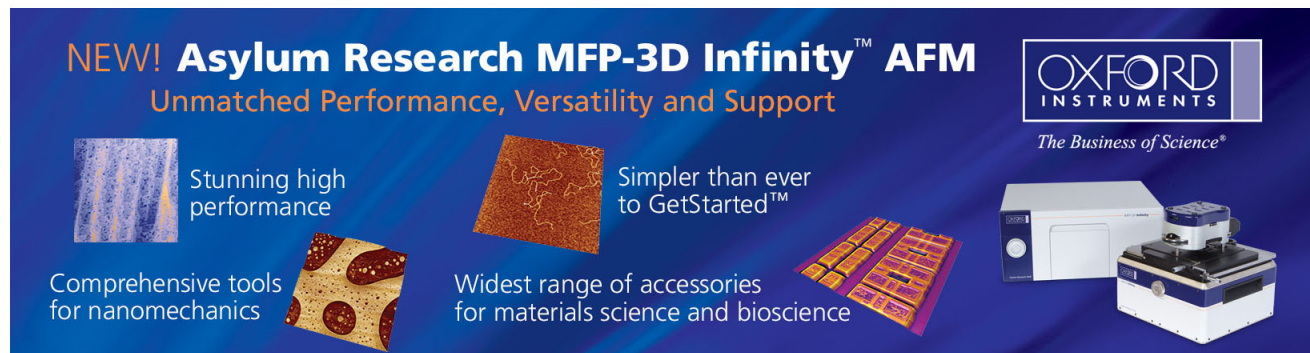
Enhanced power factor of epitaxial layered cobaltite Na_xCoO_2 thin film induced by strain: $x = 0.5, 0.7$
J. Appl. Phys. **104**, 033538 (2008); 10.1063/1.2967813

Thermopower and electrical conductivity of $\text{Mn}_{1.68-x}\text{Cu}_{0.6+x+y+z}\text{Co}_{0.24-y}\text{Ni}_{0.48-z}$ thin film oxides obtained through metal organic decomposition processing
J. Appl. Phys. **100**, 083504 (2006); 10.1063/1.2359067

Structural and transport properties of epitaxial Na_xCoO_2 thin films
Appl. Phys. Lett. **87**, 172104 (2005); 10.1063/1.2117619

Resistivity and thermoelectric power of Na_xCoO_2 ($x = 1.0, 0.7, \text{ and } 0.6$) system
J. Appl. Phys. **97**, 10A904 (2005); 10.1063/1.1847852

Characterization of epitaxial germanium grown on $(\text{La}_x\text{Y}_{1-x})_2\text{O}_3/\text{Si}(111)$ using different surfactants
J. Vac. Sci. Technol. A **23**, 448 (2005); 10.1116/1.1875253

The advertisement features a dark blue background with white and orange text. At the top left, it says 'NEW! Asylum Research MFP-3D Infinity™ AFM' in large white letters, followed by 'Unmatched Performance, Versatility and Support' in orange. On the right, the Oxford Instruments logo is shown with the tagline 'The Business of Science®'. Below the text are several images: a blue textured surface, a brown textured surface, a grid of small square samples, and the MFP-3D Infinity AFM instrument itself. Text boxes describe the 'Stunning high performance' of the instrument, its 'Simpler than ever to GetStarted™' nature, and the 'Widest range of accessories for materials science and bioscience'. A final box mentions 'Comprehensive tools for nanomechanics' with an image of a probe tip.

Fabrication and low temperature thermoelectric properties of Na_xCoO_2 ($x=0.68$ and 0.75) epitaxial films by the reactive solid-phase epitaxy

W. J. Chang,^{a)} C. C. Hsieh, T. Y. Chung, S. Y. Hsu, K. H. Wu, and T. M. Uen
Department of Electrophysics, National Chiao Tung University, Hsinchu 30010, Taiwan

J.-Y. Lin and J. J. Lin
Institute of Physics, National Chiao Tung University, Hsinchu 30010, Taiwan

C.-H. Hsu
National Synchrotron Radiation Research Center (NSRRC), Hsinchu 30076, Taiwan

Y. K. Kuo
Department of Physics, National Dong Hua University, Hualien 97401, Taiwan

H. L. Liu, M. H. Hsu, Y. S. Gou, and J. Y. Juang^{b)}
Department of Physics, National Taiwan Normal University, Taipei 10610, Taiwan

(Received 15 December 2006; accepted 4 January 2007; published online 8 February 2007)

The authors have fabricated Na_xCoO_2 thin films via lateral diffusion of sodium into Co_3O_4 (111) epitaxial films (reactive solid-phase epitaxy [Ohta *et al.*, *Cryst. Growth Des.* **5**, 25 (2005)]). The environment of thermal diffusion is key to the control of the sodium content in thin films. From the results of x-ray diffraction and in-plane ρ_{ab} , the epitaxial growth and the sodium contents of these films were identified. The thermoelectric measurements show a large thermoelectric power similar to that observed in single crystals. The quasiparticle scattering rate is found to approach zero at low temperatures, consistent with the small residual resistivity, indicating high quality of the Na_xCoO_2 thin films. © 2007 American Institute of Physics. [DOI: 10.1063/1.2437131]

The research on sodium cobaltate Na_xCoO_2 (NCO) has led to observations of many unusual physical properties exhibited in related compounds, such as the thermoelectric power,¹ charge ordered insulator at $x=0.5$,² and antiferromagnetic metal at $x=0.75$.² Furthermore, the discovery of superconductivity in $\text{Na}_x\text{CoO}_2 \cdot y\text{H}_2\text{O}$ was indeed a surprise.³ Many theoretical and experimental works have focused on the fascinating and yet puzzling ground states of NCO due to its two-dimensional triangular lattice and the mixed valence character. For the purpose of research and applications, scientists have been trying to fabricate NCO in its thin film form with modulated sodium concentrations x . Owing to the high vapor pressure of Na, however, it is difficult to directly grow high-quality epitaxial NCO thin films by pulsed-laser deposition, not to mention controlling x . Very recently, reactive solid-phase growth via lateral diffusion of sodium was reported as a viable method of growing epitaxial NCO thin films.⁴ However, precise control of sodium content and related characterizations remains to be resolved. In this letter, we report a capped-sandwich lateral diffusion scheme capable of fabricating high-quality epitaxial NCO films with well-controlled sodium contents.

In order to overcome the high vapor pressure of sodium and its associated detrimental consequences in the firsthand growth of NCO thin films, we divided the procedures of growing epitaxial NCO (0001) films into two parts. First, a layer of ~ 125 nm thick Co_3O_4 (111) thin film was deposited on sapphire (0001) substrates by pulsed-laser deposition (KrF excimer laser, $\lambda=248$ nm) with $T_{\text{substrate}}=680$ °C and $P_{\text{oxygen}}=0.2$ Torr. Subsequently, thermal-diffused sodium

was deployed to the obtained Co_3O_4 (111) to intercalate sodium into the CoO_2 layers. In our scheme, in order to keep the film surface clean and smooth during the sodium diffusion process, the Co_3O_4 (111) film was capped with a sapphire sheet as a sandwich arrangement. This fabrication process has been developed by Ohta *et al.*⁴ The process is named the reactive solid-phase epitaxy (R-SPE). For more details, see Ref. 5. In order to fabricate $\text{Na}_{0.68}\text{CoO}_2$ (NCO068) film, we used sodium carbonate powder to muffle the “sandwiched” Co_3O_4 (111) film and pressed the whole assembly into a pellet, depicted as specimen A in Fig. 1. The lateral diffusion process was carried out at 700 °C for 10 h and cooled in air with the rate <10 °C/h. For preparing the $\text{Na}_{0.75}\text{CoO}_2$ (NCO075) film, the sandwiched Co_3O_4 (111) film was first muffled by NCO075 powder obtained by rapid heat-up sintering⁶ and then encapsulated in Na_2CO_3 , as depicted schematically in Fig. 1 (specimen B). The pellet was then kept at 750–800 °C with oxygen flow for 5 h. After the

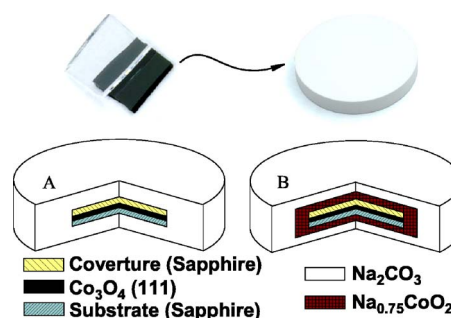


FIG. 1. (Color online) Schematics of the encapsulation schemes for preparing NCO thin films with $x=0.68$ (specimen A) and 0.75 (specimen B). The diameter of the pellets is 20 mm, and the size of the substrates is about 5×5 mm².

^{a)}Electronic mail: wei.ep90g@nctu.edu.tw

^{b)}Also at the Department of Electrophysics, National Chiao Tung University, Hsinchu 30010, Taiwan; Electronic mail: jyjuang@cc.nctu.edu.tw

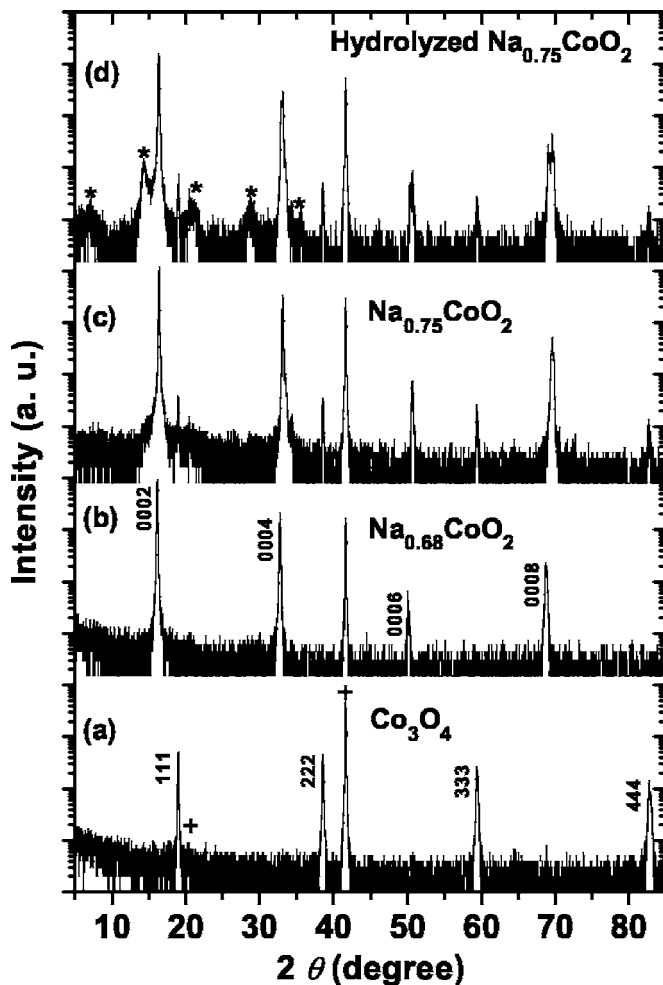


FIG. 2. XRD θ - 2θ scans of the as-grown samples of (a) Co_3O_4 , (b) NCO068, and (c) NCO075 films. (d) was measured after exposing the NCO075 film in the ambient environment at $T=25^\circ\text{C}$ and humidity of 42% for 1 h. The symbols + and * label the sapphire substrate and sodium hydroxide hydrate ($\text{NaOH}\cdot y\text{H}_2\text{O}$) peaks, respectively. The * labeled peaks of $\text{NaOH}\cdot y\text{H}_2\text{O}$ can be indexed from the database, but y is still undetermined.

lateral diffusion of sodium, the Co_3O_4 (111) films evidently converted into NCO (0001) films with the thickness expanding to ~ 250 nm.

Alternatively, Venimadhav *et al.*⁷ have used NaCOOCCH_3 powder to cover Co_3O_4 (111) films in the annealing process to obtain NCO075 films. However, there were some unsettled issues concerning the uniformity and surface quality of the films obtained by that scheme. We also had tried other process schemes to obtain specimens with $x > 0.7$. For instance, the pellet of specimen A was annealed at 800°C for a few hours then quenched immediately in liquid nitrogen from 800°C to keep as much sodium in the film as possible. However, the obtained films, though evidently displayed characteristics of NCO075, usually exhibited large residual resistivity indicating that there are more defects in the samples that presumably resulted from quenching in liquid nitrogen. In contrast, with the specimen B scheme depicted in Fig. 1, we have been able to obtain NCO075 films reproducibly with very good uniformity and surface conditions. It is suggestive from the apparent concentration of the quenched samples that, even for the scheme of specimen A, the equilibrium sodium concentration at high temperature may have reached $x \geq 0.75$ with the encapsula-

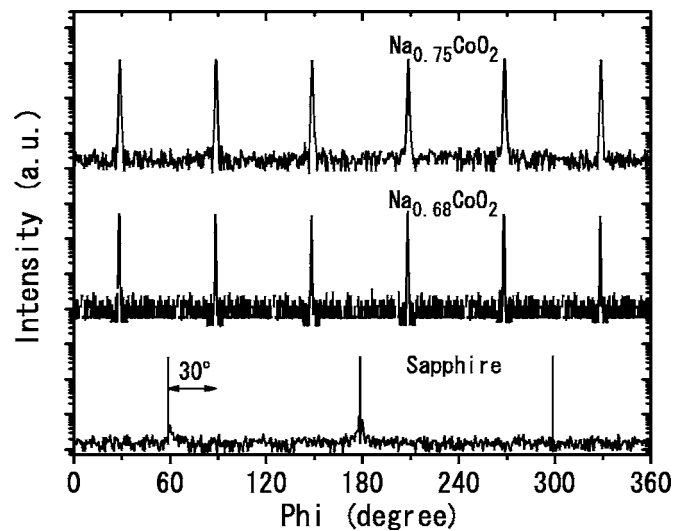


FIG. 3. Φ scans of the $(1\bar{1}04)$ peak of the NCO films and the sapphire substrate indicate the relative rotation as well as the excellent epitaxial relations between films and substrate.

tion of Na_2CO_3 powders. The slow cooling practiced in scheme A, albeit being necessary for small residual resistivity, inevitably loses some sodium and finally arrives at the stable concentration of $x=0.68$

The crystal structure and sodium concentration of NCO thin films were carefully examined by x-ray diffraction (XRD) measurements. The results of θ - 2θ and Φ scans are shown in Figs. 2 and 3, respectively. The lattice mismatch between the NCO films [$a=2.8407(2)\text{ \AA}$ for specimen A and $a=2.843(1)\text{ \AA}$ for specimen B] and the sapphire substrate ($a=4.760\text{ \AA}$) is reduced down to $\sim 3\%$ by a 30° in-plane rotation with respect to sapphire $(1\bar{1}00)$, as being illustrated in the Φ scan results of Fig. 3. The results of Figs. 2 and 3 show that Co_3O_4 (111) films were grown epitaxially on sapphire (0001) substrates, similar to the results obtained by Ohta *et al.*⁴ and Venimadhav *et al.*⁷ The NCO films obtained by both lateral diffusion schemes are also shown to be highly epitaxial to the substrate, albeit becoming (0001) oriented. Since in NCO cobaltates there exists an intimate correlation between the crystal structure parameters and Na content in the material, we inferred the Na content of the obtained NCO films by comparing the lattice constants with the structure phase diagram.⁸ From the c -axis lattice constants of specimens A [$c=10.9328(8)\text{ \AA}$] and B [$c=10.877(3)\text{ \AA}$], the inferred sodium concentrations for A and B are $x=0.68$ and 0.75 , respectively. In addition, we noted that the NCO075 films instantly react with carbon dioxide and moisture in the ambient environment resulting in loss of sodium. This behavior is reflected in the XRD results shown in Figs. 2(c) and 2(d), in which there are still traces of the Co_3O_4 (111) phase. $\rho_{\text{ab}}(T)$ is another indication of sodium loss [Fig. 4(a)] where a bended ρ - T curve characterizing NCO075 turned into a linearlike curve for NCO068 accompanied by a larger residual resistivity after a short period of exposure in air.

The $\rho_{\text{ab}}(T)$ measurements were carried out down to 0.4 K by the four-probe method. The $\rho_{\text{ab}}(T)$ curves shown in Fig. 4 display an exactly identical temperature dependent behavior to that obtained from single crystals² with similar sodium contents of $x=0.68$ and 0.75 , respectively, indicating the consistency of inferring the film composition by the

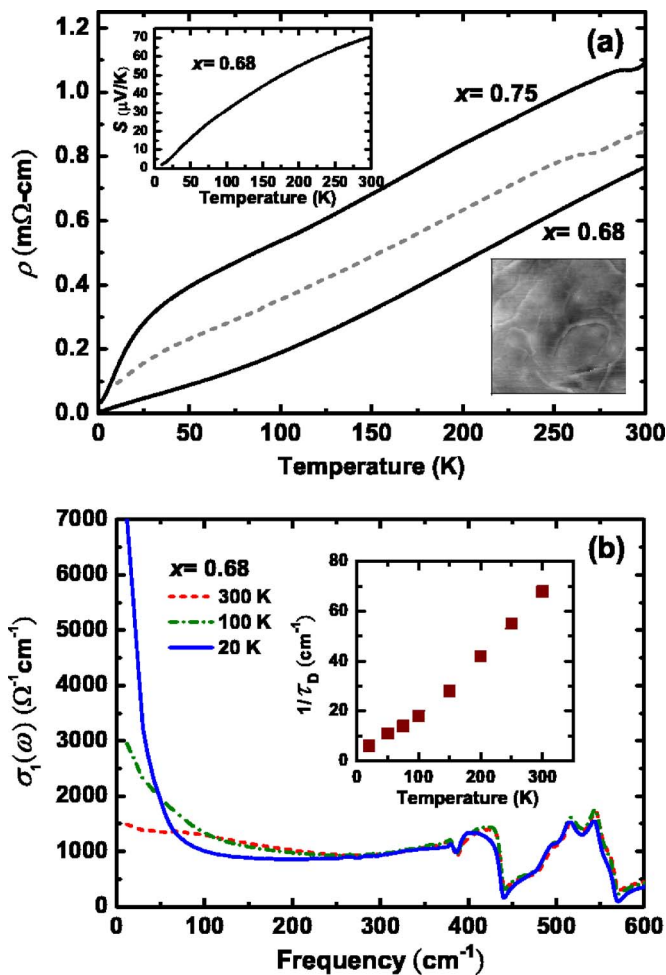


FIG. 4. (Color online) (a) In-plane resistivity ρ_{ab} vs T curves (solid lines) of NCO thin films with $x=0.68$ and 0.75 . The gray dash line illustrates the ρ_{ab} - T of hydrolyzed NCO075 in Fig. 2(d). Upper inset: $S(T)$ measurement for NCO068. Lower inset: atomic force microscopic image ($5 \times 5 \mu\text{m}^2$ and $\text{rms}=1.67 \text{ nm}$) of NCO068 thin films was measured after thermal-diffusion process. (b) Temperature dependence of the far-infrared conductivity of the NCO068 thin film. The inset shows the temperature dependence of the Drude scattering rate $1/\tau_D$.

structural and transport property comparisons. Our films notably show an even smaller residual resistivity with the residual resistivity ratios $\text{RRR} \equiv \rho(300 \text{ K})/\rho(0.4 \text{ K})=145$ and 37 , which are comparable or better than the RRR of the single crystals in Ref. 2, for $x=0.68$ and 0.75 , respectively. In addition, the ρ_{ab} - T of hydrolyzed NCO075 is illustrated by the gray dash line, which shows the characteristic of lower sodium concentration ($x < 0.75$) and larger residual resistivity. The in-plane Seebeck coefficient $S(T)$ represents yet another prominent property of this class of materials. We used a calibrated chip resistor glued to one end of the thin film as a pulsed-heat source. The temperature gradient was measured by using a differential thermocouple, and the corresponding Seebeck voltage was measured between the two signal leads connected by a pair of copper wires. The upper left inset of Fig. 4(a) shows that $S(300 \text{ K})$ is nearly $80 \mu\text{V/K}$ and is strongly temperature dependent for the NCO068, consistent with the results of single crystals in the previous literature.⁹ Unfortunately, due to the rapid deteriorating effects mentioned above, $S(T)$ for NCO075 thin films is not available yet. In any case, the results presented above

indicate that the preparation schemes in this letter can indeed produce films with very high quality.

Finally, we discuss briefly the implications of low residual resistivity at low temperatures. For this purpose, infrared spectroscopy has been proven to be the effective tool for the analysis of the transport properties of a broad range of conducting systems.¹⁰ Figure 4(b) shows the temperature dependent behavior of the far-infrared conductivity spectra for the NCO068 film. At 300 K , the low-frequency conductivity for $\omega < 100 \text{ cm}^{-1}$ can be described by a Drude peak, which grows in intensity and sharpens as the temperature is lowered. By fitting the Drude conductivity and the measured infrared reflectance self-consistently, a nearly temperature independent Drude plasma frequency $\omega_{\text{pD}} \sim 2400 \text{ cm}^{-1}$ is obtained, whereas the scattering rate $1/\tau_D$ monotonically decreases with decreasing temperature [see the inset of Fig. 4(b)]. Such behavior is typical of conventional metals.¹¹ Notably, the $1/\tau_D(20 \text{ K})$ is about 6 cm^{-1} compared with $1/\tau_D(300 \text{ K})=68 \text{ cm}^{-1}$, consistent with the small residual resistivity (or large RRR). Since the residual resistivity and $1/\tau_D(20 \text{ K})$ are proportional to the concentration of impurities or defects in the film, the transport and optical results indicate the high quality of the NCO068 thin film.

In summary, NCO thin films with $x=0.68$ and 0.75 were fabricated via R-SPE.⁴ The thin film quality is at least as decent as that of single crystals, judging from the results of XRD, $\rho_{ab}(T)$, and $S(T)$ curves. The environmental control of different equilibrium Na vapor pressures are achieved *reproducibly* by the present encapsulation schemes, which presumably have been very effective in providing sodium needed for forming NCO and at the same time preventing moisture from getting in to the films.

This work was supported by MOE ATU program and the National Science Council of Taiwan, under Grant Nos. NSC 95-2112-M-009-038-MY3, 95-2112-M-009-036-MY3, and 95-2112-M-009-035-MY3.

- ¹I. Terasaki, Y. Sasago, and K. Uchinokura, Phys. Rev. B **56**, R12685 (1997).
- ²M. L. Foo, Y. Wang, S. Watauchi, H. W. Zandbergen, T. He, R. J. Cava, and N. P. Ong, Phys. Rev. Lett. **92**, 247001 (2004).
- ³K. Takada, H. Sakurai, E. Takayama-Muromachi, F. Izumi, R. A. Dilanian, and T. Sasaki, Nature (London) **422**, 53 (2003).
- ⁴H. Ohta, S.-W. Kim, S. Ohta, K. Koumoto, M. Hirano, and H. Hosono, Cryst. Growth Des. **5**, 25 (2005).
- ⁵H. Ohta, K. Nomura, M. Orita, M. Hirano, K. Ueda, T. Suzuki, Y. Ikuhara, and H. Hosono, Adv. Funct. Mater. **13**, 139 (2003); K. Nomura, H. Ohta, K. Ueda, T. Kamiya, M. Hirano, and H. Hosono, Science **300**, 1269 (2003); K. Sugiura, H. Ohta, K. Nomura, H. Yanagi, M. Hirano, H. Hosono, and K. Koumoto, Inorg. Chem. **45**, 1894 (2006); K. Sugiura, H. Ohta, K. Nomura, M. Hirano, H. Hosono, and K. Koumoto, Appl. Phys. Lett. **88**, 082109 (2006); **89**, 032111 (2006); H. Ohta, A. Mizutani, K. Sugiura, M. Hirano, H. Hosono, and K. Koumoto, Adv. Mater. (Weinheim, Ger.) **18**, 1649 (2006).
- ⁶T. Motohashi, E. Naujalis, R. Ueda, K. Isawa, M. Karppinen, and H. Yamauchi, Appl. Phys. Lett. **79**, 1480 (2001).
- ⁷A. Venimadhav, A. Soukiassian, D. A. Tenne, Qi Lia, X. X. Xi, D. G. Schlom, R. Arroyave, Z. K. Liu, H. P. Sun, X. Pan, M. Lee, and N. P. Ong, Appl. Phys. Lett. **87**, 172104 (2005).
- ⁸Q. Huang, M. L. Foo, R. A. Pascal, Jr., J. W. Lynn, B. H. Toby, T. He, H. W. Zandbergen, and R. J. Cava, Phys. Rev. B **70**, 184110 (2004).
- ⁹Y. Wang, N. S. Rogado, R. J. Cava, and N. P. Ong, Nature (London) **423**, 425 (2003).
- ¹⁰S. V. Dordevic and D. N. Basov, Ann. Phys. **15**, 545 (2006).
- ¹¹F. Wooten, *Optical Properties of Solids* (Academic, New York, 1972), p. 42.